Atherosclerosis Amelioration by Allicin in Raw Garlic through Gut Microbiota and Trimethylamine-*N*-Oxide Modulation

Lee-Yan Sheen (lysheen@ntu.edu.tw)
National Taiwan University, Taipei, Taiwan
Suraphan Panyod
National Taiwan University, Taipei, Taiwan
Wei-Kai Wu
National Taiwan University Hospital
Pei-Chen Chen
National Taiwan University, Taipei, Taiwan
Kent-Vui Chong
National Taiwan University, Taipei, Taiwan
Yu-Tang Yang
National Taiwan University Hospital
Hsiao-Li Chuang
National Applied Research Laboratories
Chieh-Chang Chen
National Taiwan University Hospital
Rou-An Chen
National Taiwan University
Po-Yu Liu
National Taiwan University https://orcid.org/0000-0003-1290-0850
Ching-Hu Chung
Mackay Medical College
Huai-Syuan Huang
National Taiwan University
Angela Yu-Chen Lin
National Taiwan University
Ting-Chin David Shen
University of Pennsylvania
Kai-Chien Yang
National Taiwan University College of Medicine
Tur-Fu Huang

National Taiwan University College of Medicine
Cheng-Chih Hsu
National Taiwan University
Chi-Tang Ho
Rutgers University
Hsien-Li Kao
National Taiwan University Hospital
Alexander Orekhov
Skolkovo Innovative Center
Ming-Shiang Wu
National Taiwan University Hospital

Article

Keywords: cardiovascular disease, atherosclerosis, garlic juice, allicin, trimethylamine N-oxide, γ-butyrobetaine, gut microbiota

Posted Date: July 12th, 2021

DOI: https://doi.org/10.21203/rs.3.rs-519786/v1

Version of Record: A version of this preprint was published at npj Biofilms and Microbiomes on January 27th, 2022. See the published version at https://doi.org/10.1038/s41522-022-00266-3.

Abstract

Cardiovascular disease (CVD) is strongly associated with the gut microbiota and its metabolites, including trimethylamine-*N*-oxide (TMAO) formed from L-carnitine. Raw garlic juice, with allicin as its primary compound, has been shown to powerfully impact the gut microbiota. This study validated the benefits of raw garlic juice against CVD risk via modulation of the gut microbiota and its metabolites. Allicin supplementation significantly decreased serum TMAO in L-carnitine-fed C57BL/6J mice. It also reduced aortic lesions and altered the fecal microbiota in carnitine-induced, atherosclerosis-prone, apolipoprotein E-deficient mice. In human subjects exhibiting high TMAO production, raw garlic juice intake for a week reduced TMAO formation, improved gut microbial diversity, and increased the relative abundances of beneficial bacteria. In *in vitro* study, raw garlic juice inhibited γ-butyrobetaine (γBB) and trimethylamine (TMA) production by the gut microbiota. Thus, raw garlic juice can potentially prevent cardiovascular disease by decreasing TMAO production through gut microbiota modulation.

Introduction

Cardiovascular disease (CVD) is a primary cause of global mortality responsible for approximately one-third of all deaths worldwide. [1, 2] Consumption of an unhealthy diet, excessive alcohol use, smoking, and lack of physical activity are considered traditional health risk factors for CVD. [3] Recently, an insidious CVD risk factor has been explored – the gut microbiota, now considered an endocrine organ that communicates with the human body through the gut-systemic axis and extensively modifiable by foods. [4, 5, 6] The gut microbiota utilizes nutrients from undigested foods for growth and produces miscellaneous metabolites that regulate host–microbe homeostasis, which may be involved in the pathogenesis of cardiometabolic diseases. [7, 8, 9] For example, phosphatidylcholine, choline, and L-carnitine from egg, dairy products, and red meat can be metabolized by specific gut bacteria to produce trimethylamine (TMA), which is subsequently oxidized to trimethylamine N-oxide (TMAO) by hepatic flavin monooxygenase. [10, 11, 12] Increased concentrations of blood TMAO has demonstrated a strong link to increases in major adverse cardiovascular events and all-cause mortality. [13, 14] The mechanisms underlying the atherogenic and thrombogenic effects of TMAO include enhanced foam cell formation, reduced reverse cholesterol transport, and induction of platelet aggregation. [9, 10, 12, 15] TMAO has been reported to enhance platelet aggregation and induce thrombosis in both *in vitro* and human studies. [16, 17] The following multistep microbial pathway was recently proposed as the principal route for TMAO production through carnitine metabolism by the gut microbiota: L-carnitine → γ-butyrobetaine (γBB) → TMA → TMAO. [18, 19] A novel gut bacterium, *Emergencia timonensis*, was found to be capable of transforming γBB to TMA anaerobically and was reported to partially explain the phenotype of high-TMAO producers among human beings. [18, 20]

Investigations on how different food components interact with the gut microbiota have improved our understanding of modifying our dietary behaviors to achieve a health-promoting state. [8, 21] Certain approaches were proposed for reducing TMAO production by the gut microbiota such as antibiotic use,

fecal microbiota transplantation, and administration of TMA lyase inhibitor. [7, 9, 22, 23, 24] However, these approaches might exhibit safety concerns and require validation in human studies. Garlic (*Allium sativum* L.) has a long history of use as a spice in human food. [25] Traditionally, the purpose of adding garlic to meat in processed foods is not only to improve flavor but also to extend shelf life. In herbal medicine, garlic has been used as a dietary therapy against cardiovascular and other metabolic diseases. [26, 27, 28, 29] It has been widely used as a natural antibiotic on the basis of its broad-spectrum antimicrobial property. [30] Allicin is the primary compound in raw garlic puree; it is produced through the conversion of alliin by alliinase when the clove is crushed. [31] Allicin has been shown to demonstrate various antimicrobial activities in both in vitro and in vivo studies. [31, 32, 33] Recently, allicin was reported to exhibit a modulatory effect on the gut microbiota and reduced hepatic steatosis. [34, 35] Additionally, our previous pilot study showed that allicin supplementation shaped the gut microbiota composition and reduced TMAO production by the gut microbiota in mice subjected to moderate carnitine consumption (0.02 % □-carnitine). [36] However, the role of raw garlic with allicin in improving cardiovascular phenotypes via gut microbiota modulation has not been fully elucidated. Therefore, in this study, we aimed to investigate the effect of allicin and raw garlic in modulating both the function and composition of the gut microbiota for cardiovascular protection. We investigated the TMAO-reducing and gut microbiota-modulating effects of allicin in raw garlic in both rodent models and humans with higher carnitine consumption. [37] We additionally compared the anti-TMAO and anti-atherosclerotic efficacies of allicin with that of the novel TMA lyase inhibitor 3,3-dimethyl-1-butanol (DMB), [24] which has been previously shown to reduce serum TMAO in carnitine-treated mice, [17] through studies in both wild-type and apolipoprotein E-deficient ($ApoE^{-/-}$) mice. Finally, we examined the impact of allicin-containing raw garlic juice on the TMA-producing activity of the human gut microbiota and specific gut bacteria responsible for the multistep TMAO production.

Results

Allicin significantly reduced TMA and TMAO in mice, with less impact on the gut microbiome compared to □-carnitine.

To investigate the protective effect of allicin against CVD, we subjected C57BL/6J mice to increased daily consumption of □-carnitine (1.3 % in water) to examine the TMAO-reducing efficacy of allicin at a higher carnitine dosage. Additionally, we compared the TMAO-reducing effect of allicin with DMB (Fig. 1a). There was no significant change in the bodyweight of the mice (Supplementary Fig. 1). Serum TMA and TMAO were significantly reduced in the allicin-supplemented groups than in the carnitine treatment group ($P = 0.011$ and $P = 0.0008$, respectively) (Fig. 1b-c). Additionally, serum γBB was reduced in the allicin-supplemented group (Fig. 1d). According to the microbiome analysis, shift in the overall microbial composition was driven primarily by □-carnitine treatment (adonis: $P < 0.001$) (Fig. 1e), whereas the gut microbiota composition did not vary considerably among the carnitine, carnitine + allicin, and carnitine + DMB groups. Additionally, the observed operational taxonomic units (OTUs) and Chao1 index were

decreased in the □-carnitine treatment groups (P = 0.0034; P = 0.0401, respectively), whereas supplementation with allicin and DMB did not reverse the alpha diversity (Fig. 1f and Supplementary Fig. 2b). The family-level relative abundance bar plot and OTU-level heatmap supported that □-carnitine primarily shaped the gut microbiota composition with respect to specific taxa (Fig. 1g and Supplementary Fig. 2c).

Raw garlic juice reduced TMAO-producing capacity and modified the gut microbiome by enriching beneficial gut bacteria in humans.

On the basis of the TMAO-reducing effects of allicin in previous murine studies, we conducted a human pilot study to investigate whether raw garlic juice at an allicin-equivalent dosage could reduce the TMAO-producing capacity in the human body. We utilized an oral carnitine challenge test (OCCT) to evaluate TMAO-producing capacity in humans. [37] Nine volunteers were recruited to receive the OCCT, and those defined as high-TMAO producers (plasma $TMAO_{MAX} \geq 10$ μM) according to the OCCT underwent the garlic juice intervention. Among the nine volunteers, seven participants were determined to be high-TMAO producers (Plasma $TMAO_{MAX}$ = 130.91, 82.28, 57.53, 22.84, 135.62, 44.41, and 21.31 μM) (Fig. 2a and Supplementary Fig. 3a) and were allowed to proceed to the garlic juice intervention study. We first converted the allicin dose used in the murine study into a dose for humans and calculated the amount of blended garlic juice containing the equivalent dose of allicin for the interventional study. The blended raw garlic juice used in this pilot study contained 0.89 mg/mL allicin, and the participants consumed 55 mL of the prepared garlic juice per day for a week (Supplementary Fig. 4). All participants received a second OCCT after the one-week intervention. For the comparison of TMAO-producing capacity before and after the garlic juice intervention, a trend of reduced plasma $TMAO_{MAX}$ and $TMAO_{AUC}$ was observed (P = 0.051; P = 0.081) (Fig. 2b). Notably, both urine $TMAO_{MAX}$ and $TMAO_{AUC}$ were significantly reduced after the one-week garlic juice intervention (P = 0.0252; P = 0.0248) (Fig. 2c). The strong correlation between plasma and urine TMAO concentrations (Supplementary Fig. 5a) supports the use of urine samples for measuring TMAO-producing capacity. Interestingly, plasma levels of γBB in the OCCT were significantly increased (P < 0.01) (Fig. 2d), suggesting that the bioactive compounds in garlic may prevent the microbial transformation of γBB into TMA, thus decreasing TMAO formation. Our study showed a substantial reduction in platelet aggregation following the garlic juice intervention. Additionally, the maximum amplitude of platelet aggregation tended to exhibit a positive correlation with the TMAO levels (Supplementary Fig. 5b-c). Intervention with garlic juice did not lead to toxicity based on plasma biochemistry results (Supplementary Table 1). Only aspartate aminotransferase (AST) and alanine aminotransferase (ALT) were slightly increased but remained within normal range.

Overall, the gut microbial composition was not altered by the one-week consumption of garlic juice, as demonstrated through principal coordinate analysis (PCoA). The intra-individual dissimilarity in the gut microbiome before and after treatment was considerably lower than the inter-individual index (P < 0.01), suggesting that a relatively minor portion of the gut microbiota was altered by the garlic juice intervention (Fig. 2e and Supplementary Fig. 6a). Regarding the alpha diversity, garlic juice intervention significantly

increased the Shannon index (P = 0.0304) (Fig. 2f). At the family level, the fecal microbiota was altered by garlic juice; the constituent families included Acidaminococcaceae, Akkermansiaceae, Burkholderiaceae, and Erysipelotrichaceae (Fig. 2g). At the genus level, after the garlic juice intervention, the fecal microbiota of high-TMAO producers was comparatively enriched in *Akkermansia*, *Desulfovibrio*, *Lachnospiraceae UCG − 008*, *UBA1819*, and *Christensenellaceae R − 7* group (Supplementary Fig. 7). The volcano plot showed that 13 taxa were significantly altered by the garlic-juice intervention (Fig. 2h). Interestingly, certain beneficial and anti-inflammatory gut commensal bacteria, including *Faecalibacterium prausnitzii* and *Akkermansia spp.*, were significantly enriched after the one-week garlic-juice intervention ($q < 0.05$) (Fig. 2i).

Allicin ameliorated atherosclerosis, reduced TMA/TMAO production, and partially reversed the microbiome shifts in carnitine-treated ApoE $^{-/-}$ mice.

Our human study demonstrated that raw garlic juice potentially reduced TMAO production and regulated the gut microbiome by enriching beneficial gut bacteria. Thus, we further evaluated the plaque-inhibiting effects of allicin and compared it with DMB in the carnitine-induced atherosclerotic ApoE$^{-/-}$ murine model (Fig. 3a). The ApoE$^{-/-}$ mice fed □-carnitine water showed more advanced aortic plaques than the control group ($p < 0.0001$). Both allicin and DMB significantly reduced aortic plaques ($P = 0.008$ and $p < 0.0001$) (Fig. 3b-c). We additionally performed an isotope-labeled d_9-carnitine challenge test to specifically evaluate the effects of allicin on d_9-TMA/d_9-TMAO producing ability from the gut microbiota. The levels of both d_9-TMA and d_9-TMAO in the carnitine group were considerably elevated, and their area under the curve (AUC) values were significantly higher compared with that in the control group ($P = 0.0006$ and $P = 0.0008$, respectively). Both serum d_9-TMA and d_9-TMAO were substantially reduced in mice of both carnitine + allicin and carnitine + DMB groups compared with mice fed carnitine alone. Additionally, the control + allicin group showed lower d_9-TMA and d_9-TMAO levels than the control group (Fig. 3d-e). Although the carnitine + allicin treatment in the ApoE$^{-/-}$ mice showed significantly reduced atherosclerotic plaques compared with carnitine treatment alone, the reduction in TMAO-producing capacity and serum TMAO did not exhibit the expected significant difference. As this is the first time that allicin was administered to ApoE$^{-/-}$ mice over a 16-week period, we speculate that the mouse strain and treatment duration of allicin may influence the effects of allicin on TMAO reduction. Additionally, d_9-γBB, an intermediate of d_9-carnitine metabolism by gut microbiota, increased significantly in the carnitine group compared with that in the control group ($P = 0.047$), which is consistent with the result from our previous human study (Fig. 3f and Fig. 2c). Interestingly, the carnitine + allicin and carnitine + DMB groups showed greater elevation in serum d_9-γBB than the carnitine group, which indicates that the process of d_9-γBB transformation into downstream TMA might be inhibited, leading to the buildup of d9-γBB.

We subsequently investigated the alteration in gut microbiome composition in different treatment groups through 16S rRNA sequencing analysis with the QIIME pipeline. Regarding the beta-diversity, the PCoA showed that carnitine water induced a significant microbiome shift (especially at the PCoA2 axis) that was partially reversed by treatment with allicin and DMB (adonis: $P < 0.001$) (Fig. 3h). Regarding the □-

diversity, carnitine water alone exhibited decreased observed OTUs, the Shannon index, and the Chao1 index (P = 0.0004; P < 0.001; P = 0.0063 respectively), whereas additional treatment with allicin or DMB showed favorable alpha-diversity indices (Fig. 3g). A heatmap of the gut microbiome demonstrated differences in the fecal microbiome (Fig. 3i); the carnitine + DMB group exhibited enrichment in certain beneficial bacteria, including *Roseburia and Akkermansia*, which have been reported to correlate inversely with atherosclerotic lesions and protect against atherosclerosis. [38, 39] However, in the □-carnitine + allicin group, the relative abundances of these bacteria were reduced compared to that in the □-carnitine + DMB group, suggesting that allicin might exert bactericidal activity against these beneficial bacteria and limit improvement in atherosclerotic plaques compared to the □-carnitine + DMB group.

Raw garlic juice inhibited microbial carnitine → γBB → TMA pathways in vitro

Our study showed that raw garlic juice reduced TMAO-producing capacity through carnitine metabolism in TMAO-producing participants, C57BL/6J mice, and aortic lesion-exhibiting ApoE$^{-/-}$ mice. However, it is unknown whether it can specifically inhibit microbial pathways of carnitine metabolism. Thus, we subsequently conducted an in vitro study to examine the inhibitory effects of raw garlic juice on the following pathway: carnitine → γBB → TMA (Fig. 4a). In functional assays, we used fecal samples from the high-TMAO producers and documented strain types responsible for the following pathways: carnitine → γBB and γBB → TMA.

We standardized the functional assay to examine inhibition of the following pathway: carnitine → γBB → TMA. For this purpose, we established a simplified model by co-culturing type strains that have been reported to metabolize carnitine to form γBB, including *Proteus penneri*, *Escherichia fergusonii*, and *Edwardsiella tarda*. The three co-cultured bacterial strains were inoculated in Wilkins–Chalgren (WC) broth supplemented with d_9-carnitine. The concentration of garlic juice was titrated to a potent inhibitory level in the incubation broth. Raw garlic juice at 5 % and 10 % exhibited potent inhibition of the transformation of d_9-carnitine into d_9-γBB (Fig. 4b). Single type strain experiments showed consistent results (Supplementary Fig. 10). *E. timonensis* is a novel bacterium isolated from the human gut; it was recently reported to metabolize γBB to TMA. We observed that raw garlic juice exhibited potent inhibition of d_9-TMA production by *E. timonensis* using d_9-γBB as a substrate at 0.6 % garlic juice, which is a relatively low concentration of the prepared garlic juice (Fig. 4c).

To test the inhibitory effect of garlic juice in a complex microbiome community, we collected the feces from high-TMAO producing participants and cultured in WC broth supplemented with d_9-carnitine or d_9-γBB. WC broth supplemented with d_9-carnitine inoculated with feces from high-TMAO producers showed that the d_9-γBB level was the highest at 6 h while d_9-TMA was not detected at that time point. At 12 h, the d_9-γBB level was reduced with simultaneous formation of d_9-TMA. Raw garlic juice at 5 % and 10 % concentrations in the culture medium showed optimal inhibition of TMA formation with moderate bacterial growth inhibition (Fig. 4d). d_9-γBB started to be utilized to form d_9-TMA over 6 to 12 h in broth

supplemented with d_9-γBB. Similarly, 5 % and 10 % garlic juice were determined to be an optimal concentration for preventing fecal microbiota from utilizing d_9-γBB to form d_9-TMA (Fig. 4e).

Discussion

Allicin supplementation in C57BL/6J mice fed a high concentration (1.3 %) of □-carnitine demonstrated that the primary compound in raw garlic juice, allicin, potentially inhibited the gut microbiota– and liver-derived TMA and TMAO in circulation, which is consistent with the results of our previous study, in which mice were administered a daily dosage (0.02 %) of □-carnitine. [36] In the murine study, □-carnitine intake was the principal factor affecting the overall gut microbiota composition compared with allicin or DMB intervention. The TMAO-reducing effect of allicin is probably based on its broad-spectrum antimicrobial activities. [31] Additionally, previous studies reported that garlic and its bioactive compounds exhibited lipid-lowering and fatty liver-protective effects via gut microbiota modulation. [35, 40] Following allicin intake, it can be metabolized to various sulfur-containing bioactive compounds, such as diallyl sulfide, diallyl disulfide, and diallyl trisulfide for modulating the microbiome composition in the gut. [41, 42, 43, 44]

Previously, in a human study, we developed the OCCT, which can robustly distinguish the low- and high-TMAO producers. [37] In this study, high-TMAO producers were defined as individuals exhibiting OCCT plasma $TMAO_{MAX}$ level ≥ 10 μM [20]. There is currently a lack of studies on the effect of garlic on the gut microbiota in the human body; this study is the first to demonstrate the impact of garlic on TMAO production by the gut microbiota. In this human study, after the intake of garlic juice for one week, both plasma and urine TMAO were reduced, suggesting that the bioactive compounds in garlic inhibited gut microbial carnitine utilization and TMA-formation ability, resulting in reduction of TMAO. The current study demonstrated that plasma and urine TMAO exhibited a high positive correlation that was consistent with the results from previous studies. [20, 37] Currently, the primary genes responsible for converting carnitine to TMA by the gut microbiota remains unclear. A Rieske-type microbial *CntA/B* enzyme was reported to convert carnitine to TMA. [15] However, it is doubtful whether *CntA/B* is responsible for TMA formation in the gut anaerobic environment because oxygen is required for its reaction. [18, 37] A recent study showed that □-carnitine can be metabolized to the intermediate γBB, followed by transformation into TMA via a low-abundance anaerobic bacterium called *E. timonensis*; this could be the major pathway for TMA generation by the gut microbiota in the oxygen-limited environment. [18] This study showed an increase in plasma γBB following the garlic-juice intervention, suggesting that garlic juice might block the conversion of γBB to TMA, resulting in accumulation of γBB.

The gut microbiome analysis showed that the garlic-juice intervention increased the Shannon index, indicating that a more diverse and balanced microbial community was produced by garlic-juice consumption. The overall gut microbiome profile for each individual was moderately affected by the garlic-juice intervention; however, the relative abundances of certain beneficial gut bacteria were increased following garlic-juice intake, including *Akkermansia*, Lachnospiraceae, Christensenellaceae, and *Faecalibacterium prausnitzii*. *Akkermansia muciniphila*, a mucin-degrading bacterium that resides in

the mucus layer, has been demonstrated to be inversely associated with obesity and type 2 diabetes. Prebiotic administration with *Akkermansia* improves the metabolic profile and reduces metabolic disorders, obesity, endotoxemia, adipose tissue inflammation, and insulin resistance. [45] *A. muciniphila*-derived extracellular vesicles improve gut permeability through the regulation of tight junctions, as well as decrease body weight gain and reduce glucose tolerance in high-fat diet-induced diabetic mice. [46] Furthermore, it shields against atherosclerosis by blocking metabolic endotoxemia-induced inflammation in ApoE$^{-/-}$ mice. [39] The garlic intervention increased the level of *Faecalibacterium pranusnitzii*, which has been reported to be an anti-inflammatory commensal bacterium that secretes a metabolite blocking NF-κB activation and IL-8 secretion. [47] These results suggested that the garlic-juice intervention modulates the gut microbiota of high-TMAO producers in a favorable direction. However, drinking raw garlic juice on an empty stomach may cause abdominal discomfort, and thus it should be consumed with a meal to prevent undesirable stomachache.

In ApoE$^{-/-}$ mice, 1.3 % γ-carnitine induced atherosclerosis that was ameliorated by allicin supplementation, indicating the potential anti-atherosclerotic activity of allicin. However, we observed that TMAO inhibition by allicin was more effective with short-term treatment in C57BL/6J mice than with long-term treatment in ApoE$^{-/-}$ mice, which suggested that long-term allicin administration could result in the resistance of TMA-producing bacteria against the anti-microbial effect of allicin. However, long-term allicin administration resulted in more differences in the overall gut microbiota in ApoE$^{-/-}$ mice. The allicin and DMB group with γ-carnitine group in the long-term study exhibited a similar gut microbiota composition. Additionally, the in vitro study suggested that garlic inhibited the formation of both d_9-γBB and d_9-TMA in the culture medium inoculated with the co-culture of bacteria producing γBB (*P. penneri*, *E. fergusonii*, and *E. tarda*) and TMA (*E. timonensis*), as well as inhibited TMA formation by the complex bacterial consortium of the TMAO-producing microbiota.

Here, we demonstrated that supplementation with allicin inhibited TMAO production through carnitine metabolism by the gut microbiota in both mice and humans and prevented carnitine-induced atherosclerosis in ApoE$^{-/-}$ mice. This was supported by in vitro assays using specific bacteria that metabolize γ-carnitine to γBB and γBB to TMA (Fig. 5). These data provide valuable evidence that raw garlic, which contains allicin, shifts the gut microbiota composition and modulates the following gut microbial pathway: γ-carnitine → γBB → TMA. In summary, this study suggests that garlic might serve as a potential dietary intervention for CVD prevention.

Methods

Allicin preparation for the animal study.

Allicin synthesis, purification, and identification were based on our laboratory protocol. [35, 36, 48] The purity of allicin was more than 97 %; it was dissolved in 0.5 % carboxymethyl cellulose (CMC) and stored at −80 °C before administration to the mice.

-carnitine-fed C57BL/6J mouse model.

The handling of animals complied with the guidelines of the Institutional Animal Care and Use Committee of National Taiwan University (approval number: NTU107-EL-00170 and NTU107-EL-00084). Six-week-old male C57BL/6J mice were purchased from Taiwan National Laboratory Animal Center. The mice were housed in a room with a 12 h light–dark cycle at 22 ± 2 °C after an adaptation period of 2 weeks. The mice were randomly divided into experimental groups (i) control; (ii) control + allicin; (iii) carnitine; (iv) carnitine + allicin; and (v) carnitine + DMB. For the carnitine intake group, 1.3 % -carnitine in water was supplied. [10] Allicin treatment groups were orally administered 10 mg/(kg bw day) allicin in 0.5 % CMC. [36] The DMB group was treated with 1 % DMB in water. [24] The mice were sacrificed by CO_2 asphyxiation after two weeks. Blood was collected from the major arteries of the abdomen using a syringe.

Long-term -carnitine-induced atherosclerosis ApoE$^{-/-}$ mouse model.

The ApoE$^{-/-}$ mice were initially purchased from the Jackson Laboratory (Bar Harbor, ME) and bred in our laboratory animal room according to the guidelines of the Institutional Animal Care and Use Committee of National Taiwan University. Six-week-old female ApoE$^{-/-}$ mice were utilized for the experiment after an adaptation period of 2 weeks. The mice were grouped and treated similarly to the short-term C57BL/6J mouse model, as described previously. The ApoE$^{-/-}$ mice were sacrificed after 15 weeks. Blood was collected from the major arteries of the abdomen using a syringe. Phosphate-buffered saline (PBS) was used to gently flush the aorta to remove blood clots, and the aorta was removed from the body.

Oral d_9-carnitine challenge test in the mouse.

On the day of the sacrifice, the mice were gavaged with 200 μL (150 mM) of d_9-carnitine, followed by serial blood collection at 0, 4, 8, and 10 h. [36] Subsequently, the mice were subjected to carbon dioxide asphyxiation. Blood was collected from the major arteries of the abdomen using a syringe at 12 h. The blood samples were centrifuged at 1,000 × *g* for 15 min. The supernatants were collected and stored at −80 °C before further analysis.

Oil red staining of the aorta

Aortic specimens were rinsed with PBS to remove excess blood residue. Dissection was performed under the microscope using micro-dissection scissors and forceps to remove the adipose tissue. The aorta was fixed with 10 % formalin and stained with oil red O dye [49] as follows: it was (1) washed with deionized water for 5 min; (2) soaked in propylene glycol for 10 min; (3) stained with oil red O dye; (4) soaked in 85 % propylene glycol for 3 min; and (5) washed twice with deionized water. We captured images of the stained aorta and analyzed the aortic lesion area using the Image J software (Version 1.8.0).

Mouse blood biochemistry analysis

The serum was extracted via centrifuging the blood at 1,000 × *g* for 15 min at 4 °C. We analyzed serum biochemical parameters, including total cholesterol, total triglyceride, high-density lipoprotein (HDL-c), AST, and ALT, using commercial test strips (Spotchem II reagent strips; Arkray Inc., Kyoto, Japan) in an automatic blood analyzer (Spotchem EZ). [50]

High-TMAO producer screening by OCCT.

This research was approved by the Research Ethics Committee of National Taiwan University Hospital (201712031RIND), and the study has been registered on ClinicalTrials.gov as NCT04545879. Healthy participants were recruited (n=9), under the following criteria: (1) age ≥ 20 years old; (2) no exposure to antibiotics, probiotics, or carnitine supplements within the previous month; (3) no history of chronic diseases including, diabetes mellitus, myasthenia gravis, chronic renal disease, hyperparathyroidism, epilepsy, and severe anemia; (4) Participants were excluded from the study if they reported recent gastrointestinal discomfort (such as abdominal pain or diarrhea).

We used the OCCT, which was previously shown to exhibit better efficacy than fasting plasma TMAO, to identify the TMAO producer phenotype. [37] All participants fasted at least 8 h before the OCCT. The participants were orally administered 1,500 mg of □-carnitine (3 tablets, General Nutrition Centers, Inc., USA). The blood and urine of the participants were collected at 0, 24, 48, and 72 h after carnitine intake. The plasma and urine samples were centrifuged at 1,000 × *g* for 15 min and stored at −80 °C before the following analyses. Participants with plasma TMAO ≥ 10 μM after the OCCT were defined as high-TMAO producers and allowed to proceed for the garlic juice intervention. [20]

Garlic juice preparation and allicin content quantification

Raw garlic was peeled to remove the skin; 100 g of garlic and 300 mL of water (ratio 1:3) were mixed and blended into garlic juice using a blender. After filtration, the raw garlic juice was placed into a glass bottle (55 mL for each), ready to be consumed by the subjects. The garlic juice required was prepared at once and frozen at −20 °C before use.

The allicin content in the raw garlic juice was determined using HPLC (JASCO LC-NetII/ADC/JASCO UV-2075 Plus) with Shiseido C18 (5 μm, 4.6 mm × 250 mm). The mobile phase was deionized water and methanol, and the flow rate was 1 mL/min. The gradient program was run as follows: 0–100 % methanol, 0–30 min and 100 % methanol, 10 min. The absorbance was detected at 254 nm. The allicin concentration in raw garlic juice was calculated against the allicin standard curve at concentrations of 0.2, 0.4, 0.6, 0.8, and 1.0 mg/mL.

Garlic Juice Intervention

High-TMAO producers (n=7) were asked to consume 55 mL of raw garlic juice (48 mg of allicin equivalent) once a day during dinner for one week. High-TMAO producers were suggested to consume the garlic juice with a meal to decrease stomach irritation caused by quick drinking of raw garlic juice. The

high-TMAO producers were free to choose their diet with no restriction on the type of food. After one week of raw garlic juice intervention, the second OCCT was performed.

Gut microbiota inoculum preparation from human feces for in vitro study

We mixed 1 g of raw fecal sample with 10 mL of PBS supplement with 0.05 % L-cysteine in a tube containing glass beads, homogenized the mixture by vortexing for 1 min in an anaerobic chamber (Whitley DG250 Workstation, Don Whitley Scientific Limited, UK), filtered the homogenized fecal liquid through a Falcon® 100 µm cell strainer, and subsequently used the fecal filtrate for the study.

Media selection study for maximal TMA production

To investigate the suitability of the culturing media for producing maximal TMA concentration, we compared three media: gut microbiota medium (GMM), [51] MEGA, [52] and WC medium. [53] Furthermore, we modified these media as a carbon-reduced medium. The media were supplemented with 100 µM L-carnitine. The media recipes are provided in the Supplementary Tables 2–4. Two gut microbiota inocula from the feces of high-TMAO producers were prepared by mixing 1 g of feces with 15 mL of PBS with 0.05 % cysteine and filtering the mixture through a 100 µm Falcon cell strainer, following which 100 µL of the stool filtrate was transferred to 1.9 mL of medium and subsequently incubated at 37 °C under anaerobic conditions (80 % N_2, 10 % CO_2, and 10 % H_2) for 0, 6, 12, and 24 h. The cultures were collected, their growth measured at optical density (OD) 600 nm (Spectronic Helios Gamma UV-Vis Spectrophotometer, Thermo Fisher Scientific, UK), centrifuged at 6,000 rpm for 1 min, and the supernatant collected for measuring TMA, TMAO, γBB, carnitine, and choline concentration using LC-MS.

Gut microbiota inoculum and bacteria

The medium used in this study was WC broth supplemented with d_9-carnitine or d_9-γBB. We used the WC broth because it produces the highest TMA level compared with GMM, the MEGA medium, and its carbon-reduced medium (Supplementary Fig. 9). The high-TMAO producer stool for the inhibition study was re-collected from the participant (GJ07), which exhibited the highest $TMAO_{MAX}$ during the OCCT and possessed the *E. timonensis* 16S sequence in the sample. The bacteria used in this study include the bacteria responsible for converting L-carnitine to γBB *P. penneri* ATCC33519, *E. fergusonii* ATCC35469, and *E. tarda* ATCC15947. [54] *E. timonensis* DSM101844 transforms γBB to TMA. [18] A single colony on the WC agar plate of the bacteria was inoculated into the WC broth for 24 h under anaerobic conditions before being used in the inhibition study.

Inhibition study of raw garlic juice against high-TMAO producer gut microbiome and γBB/TMA-producing bacteria

Garlic juice was prepared as described above, following which it was sterilized by filtration through 0.22 µm polyvinylidene fluoride membranes. We inoculated 50 µL of the gut microbiota inoculum from the high-TMAO producers, which was prepared as described above, in 1 mL of WC broth with 50 µM d_9-

carnitine or d_9-γBB. Subsequently, the sterilized raw garlic juice was added at final concentrations of 0, 0.3, 0.6, 1.3, 2.5, 5.0, and 10.0 % and incubated at 37 °C under anaerobic conditions (80 % N_2, 10 % CO_2, and 10 % H_2) for 0, 6, 12, and 24 h. We collected the cultures, estimated the growth OD_{600}, centrifuged the cultures at 6,000 rpm for 1 min, and collected the supernatant for measuring d_9-TMA, d_9-γBB, and d_9-carnitine using LC-MS. For evaluating the inhibition of bacteria related to CVD, the γBB-producing bacteria *P. penneri*, *E. fergusonii*, and *E. tarda* were mixed before the inhibition analysis. We inoculated 100 µL of the γBB-producing bacterial mixture in 1 mL of WC broth with 100 µM d_9-carnitine, added garlic juice, cultured the bacteria, and performed the analysis as mentioned above. For analyzing the inhibition of *E. timonensis*, we inoculated 100 µL of the inoculum in 1 mL of WC broth with 100 µM d_9-γBB, added the garlic juice, cultured the bacteria, and performed the analysis as mentioned above.

Measurement of the concentration of TMA, d_9-TMA, TMAO, d_9-TMAO, gBB, d_9-gBB, carnitine, d_9-carnitine, and choline by LC-MS.

Sample preparation and quantification of TMA, TMAO, gBB, carnitine, d_9-TMA, d_9-TMAO, d_9-gBB, d_9-carnitine in mice

For sample preparation, 50 µL of mouse serum was added to 450 µL of methanol containing isotopically labeled internal standards (d_3-carnitine, d_9-TMAO, and $^{13}C_3$-TMAO). Subsequently, the mixture was centrifuged at 12,000 × *g*, 4 °C for 5 min, and the supernatants were collected for LC-MS.

For LC-MS analysis, the target metabolites of the serum samples were analyzed using the Agilent 1290 UHPLC tandem Agilent 6460 triple quadrupole mass spectrometer. The MicroSolv Cogent Diamond Hydride column (150 × 2.1 mm, 4.2 µm, MicroSolv, Eatontown, NJ) was used in this study by maintaining the column temperature at 40 °C. Mobile phase solution A was 10 mM ammonium acetate, 0.2 % formic acid in deionized water; solution B was 10 mM ammonium acetate and 0.2 % formic acid in 90 % acetonitrile. The flow rate was 0.4 mL/min, and the gradient program was as follows: 90–75 % solution B for 0–1 min; 75–65 % solution B for 1–2 min; 65–55 % solution B for 2–4 min; 55–40 % solution B in 4–5 min, followed by re-equilibration of the column with 90 % solution B for 1 min.

For MS, the positive electrospray ionization mode was used with the following parameters: drying gas temperature was set at 325 °C, flow rate 7 L/min, nebulizer pressure at 45 psi, sheath gas temperature at 325 °C, 11 L/min sheath gas of flow rate, the capillary voltage at 3,500 V, and nozzle voltage at 500 V. The mass spectrometer was configured in multiple reaction monitoring mode. The monitored transitions for carnitine were: m/z 162.1 → 43.2 and 162.1 → 60.2; d_3-carnitine, m/z 165.1 → 43.1 and 165.1 → 61.2; TMAO, m/z 76.1→58.1 and 76.1→59.1; d_9-TMAO, m/z 85.1→66.3 and 85.1→68.3; $^{13}C_3$-TMAO, m/z79.1→61.1 and 79.1→62.1; TMA, m/z 60.1→45.2 and 60.1→44.1; d_9-TMA, m/z 69.1→51.1 and 69.1→49.1; and $^{13}C_3$-TMA, m/z 63.1→46.1. The detected peak area ratio was used to calculate the concentration of each target analyte in the serum sample against the calibration curve.

Sample preparation and quantification for TMA, TMAO, gBB, carnitine, choline, d_9-TMA, d_9-TMAO, d_9-gBB, d_9-carnitine in human and culture medium

For sample preparation. 1 µL of plasma, urine, or culture medium was mixed with 199 µL of isotopically labeled internal standards (d_3-carnitine, d_9-TMAO, and $^{13}C_3$-TMAO) in 0.1 % formic acid acetonitrile solution. The solution was subsequently centrifuged at 15,000 rpm, 0 °C for 5 min. For urine sample preparation, the urine was first centrifuged at 3,000 × *g*, 22 °C for 15 min. We mixed 5 µL of the 1st supernatant obtained with 45 µL of isotopically labeled internal standards (d_3-carnitine, d_9-TMAO, and $^{13}C_3$-TMAO) in 0.1 % formic acid acetonitrile solution. The solution was centrifuged at 15,000 rpm, 0 °C for 5 min, and the 2nd supernatant was obtained. Next, 2 µL of the 2nd supernatant was mixed with 198 µL of internal standard and centrifuged at 15,000 rpm, 0 °C for 5 min; the supernatant obtained was ready for LC-MS/MS quantification. The prepared plasma and urine samples were analyzed using LC-MS/MS SCIEX 5500 for TMA, TMAO, gBB, carnitine, and choline quantification.

For LC-MS/MS analysis, 20 µL of each plasma or urine sample was injected into a Sciex Exion LC AC system coupled with a SCIEX Triple TOF 5600 mass spectrometer (AB SCIEX, Canada). The separation was performed using an HILIC column (250 × 4.0 mm, 5 µm, Fortis, UK) maintained at 40 °C. Mobile phase A was 0.1 % formic acid in deionized water, and mobile phase B was 0.1 % formic acid in acetonitrile. The flow rate was 0.5 mL/min. The LC program: 0–1 min, 50 % solvent B, 1–9 min, 50–40 % solvent B, 9–10 min, 40 % solvent B, 10–10.1 min, and 40–50 % solvent B, followed by column re-equilibration with 50 % solvent B for 1.9 min. The electrospray was set in positive ionization mode with the following parameters: curtain gas supply, 30 psi; capillary temperature, 500 °C; spray voltage floating, 5,500 V; and declustering potential, 80 V. The concentration of each analyte was calculated from calibration curves relating the peak area ratio to its corresponding standard.

Platelet Preparation and Aggregometry Assays

Platelet preparation and aggregometry assays were performed according to the methods used by Zhu et al. (2016) with modifications. [16] Whole blood was collected from study participants using 3.2 % sodium citrate anticoagulant. Platelet-rich plasma (PRP) was obtained by centrifugation at 100 × *g*, 22 °C for 6 min. Platelet poor plasma (PPP) was prepared by further centrifugation at 11,000 × *g* for 2 min. Platelets were counted using Sysmex K1000 Hematology Analyzer, and the CHRONO-LOG490-4D system was used for aggregometry assays. Platelet concentrations were adjusted to 2 × 108/mL with PPP. 5 µM ADP was used as indicated to initiate aggregation with constant stirring (600 rpm). Both PRP and PPP samples were kept at 37 °C before the aggregometry assays were performed.

Fecal DNA Extraction and 16S rRNA amplicon sequencing and sequencing analysis

Fecal sample collection and genomic DNA extraction

Mouse fecal samples were collected from the large intestine during a sacrifice from both the long-term study in -carnitine-induced ApoE$^{-/-}$ mice and short-term study in the C57BL/6J experimental mouse model; the samples were snap frozen using liquid nitrogen and stored at −80 °C before use. Human fecal samples were collected before and after the garlic juice intervention using a stool collection kit. [55] The samples were stored at −80 °C for further examination. Fecal genomic DNA was extracted using the QIAmp Power Fecal DNA Kit (QIAGEN, Netherlands) according to the manufacturer's instructions and quantified using the NanoDrop ND-1000 spectrophotometer (Thermo Fischer Scientific).

Polymerase Chain Reaction (PCR), Library Preparation, and 16S rRNA Gene Sequencing

The V3-V4 hypervariable region of the 16S rRNA gene was amplified using the primer pair ((Forward = 5'-TCG TCG GCA GCG TCA GAT GTG TAT AAG AGA CAG CCT ACG GGN GGC WGC AG-3') and Reverse = 5'-GTC TCG TGG GCT CGG AGA TGT GTA TAA GAG ACA GGA CTA CHV GGG TAT CTA ATC C-3')). PCR amplification was performed in a 25 µL reaction mixture containing 5 ng of DNA template, 0.2 µM forward and reverse primers, and 12.5 µL of 2× Taq Master Mix (KAPA HiFi HotStart ReadyMix, Roche, Switzerland). The PCR conditions involved an initial step at 95 °C for 3 min, followed by 25 cycles of 95 °C for 30 s, 55 °C for 30 s, 72 °C for 30 s, and a final extension of 72 °C for 5 min. Subsequently, 2 % agarose gel electrophoresis was used to visualize the amplified products. Dual index and Illumina sequencing adapters were attached by using a Nextera XT Index Kit via PCR according to the manufacturer's instructions. PCR product cleanup was conducted using AMPure XP beads to purify the V3-V4 amplicon. The sizes of PCR products were confirmed using the Bioanalyzer DNA 1000 chip. Library quantification was conducted for quality control before sequencing using the Agilent Technologies 2100 Bioanalyzer. The pooled libraries were subjected to paired-end sequencing (2 × 300 bps) using the Illumina MiSeq platform.

Sequencing Analysis

The raw sequences were processed following the instructions in the 16S Bacteria/Archaea SOP v1 of the Microbiome Helper workflows (https://github.com/mlangill/microbiome_helper). [56] The paired-end reads were filtered as a sequence length of over 400 and a quality score of 90 % at a Phed score 30, followed by the removal of the chimeric sequences using VSEARCH v2.1.2. [57] The high-quality reads were subsequently analyzed using QIIME v.1.9.1. [58] OTUs were produced using the UCLUST algorithm and a closed-referenced OTU approach against the SILVA database (version 132) with 97 % of sequence identity, followed by rarefaction. The vegan package in R was used to calculate α-diversity indices, including the observed OTUs, Shannon index, and Chao1 index, PCoA based on the Bray–Curtis distance. We performed permutation multivariate analysis of variance (ANOVA) using distance matrices (adonis) to determine the heterogeneity of the fecal microbiota among the groups. A heatmap was plotted using the heatmap3 package.

Statistical Analysis

Data are represented as the mean ± standard error of the mean (SEM) or mean ± standard deviation. An unpaired two-tailed Student's t-test or one-way ANOVA with Tukey's range test was used to compare group means in an animal study. For the human study, data are expressed as the mean ± SEM; paired two-tailed Student's t-test was used to compare the difference between before and after garlic juice intake. The Kruskal–Wallis test, Wilcoxon signed-rank test with or without false discovery rate, unpaired/paired two-tailed Student's t-test, and one-way ANOVA with Tukey's range test were used for the analysis of the fecal microbiome data based on the data set. All statistics were analyzed using Graphpad Prism (version 8.4.3), R (version 3.6.1), or R Studio (version 1.2.5001).

Declarations

Data availability

The raw 16s rRNA sequencing data used to produce all figures are accessible at the NCBI Short Read Archive under the following accession numbers: BioProject: PRJNA661156 and SRA: SRS7316558, SRS7317051, and SRS7315455.

Acknowledgements

This study was financed by the Ministry of Science and Technology (Taiwan) (107-2321-B-002-017, 108-2321-B-002-035, 107-2321-B-002-039, and 108-2321-B-002-051).

Author contributions

S.P. instructed and assisted the experiment, performed the bioinformatics and statistical analysis, and drafted the manuscript; W.K.W. designed and instructed the animal and human experiments; K.V.C. performed the human and in vitro studies; P.C.C. performed the animal experiments; Y.T.Y. conducted the PCR and library preparation for 16S rRNA gene sequencing; H.L.C. guided the animal studies; C.C.C. assisted the human study; R.A.C. and H.S.H. assisted the human study and animal experiments; P.Y.L. assisted the bioinformatics analysis; C.H.C. assisted platelet preparation and aggregometry assays; A.Y.C.L. and C.C.H. instructed target metabolomics analysis and assisted with mass spectrometry analysis; K.C.Y. and T.F.H provided the technical support in the $ApoE^{-/-}$ experiment and aortic lesion investigation; T.C.D.S., H.L.K., C.T.H. and A.N.O. critically reviewed the manuscript; M.S.W. and L.Y.S. designed the experiments, provided the funding for the study, and critically revised the manuscript.

Competing interests

The authors declare that there are no competing interests.

References

1. Roth, G. A. et al. Global, regional, and national burden of cardiovascular diseases for 10 causes, 1990 to 2015. *J. Am. Coll. Cardiol.* **70**, 1-25 (2017).

2. Zhao, D., Liu, J., Wang, M., Zhang, X. & Zhou, M. Epidemiology of cardiovascular disease in china: Current features and implications. *Nat. Rev. Cardiol.* **16**, 203-212 (2019).

3. Noble, N., Paul, C., Turon, H. & Oldmeadow, C. Which modifiable health risk behaviours are related? A systematic review of the clustering of smoking, nutrition, alcohol and physical activity ('snap') health risk factors. *Prev. Med.* **81**, 16-41 (2015).

4. Clarke, G., Stilling, R. M., Kennedy, P. J., Stanton, C., Cryan, J. F. & Dinan, T. G. Minireview: Gut microbiota: The neglected endocrine organ. *Mol. Endocrinol.* **28**, 1221-1238 (2014).

5. David, L. A. et al. Diet rapidly and reproducibly alters the human gut microbiome. *Nature* **505**, 559-563 (2014).

6. Jie, Z. et al. The gut microbiome in atherosclerotic cardiovascular disease. *Nat. Commun.* **8**, 845 (2017).

7. Brown, J. M. & Hazen, S. L. The gut microbial endocrine organ: Bacterially derived signals driving cardiometabolic diseases. *Annu. Rev. Med.* **66**, 343-359 (2015).

8. Gentile, C. L. & Weir, T. L. The gut microbiota at the intersection of diet and human health. *Science* **362**, 776-780 (2018).

9. Witkowski, M., Weeks, T. L. & Hazen, S. L. Gut microbiota and cardiovascular disease. *Circ. Res.* **127**, 553-570 (2020).

10. Koeth, R. A. et al. Intestinal microbiota metabolism of l-carnitine, a nutrient in red meat, promotes atherosclerosis. *Nat. Med.* **19**, 576-585 (2013).

11. Tilg, H. A gut feeling about thrombosis. *New Engl. J. Med.* **374**, 2494-2496 (2016).

12. Wang, Z. et al. Gut flora metabolism of phosphatidylcholine promotes cardiovascular disease. *Nature* **472**, 57-63 (2011).

13. Schiattarella, G. G. et al. Gut microbe-generated metabolite trimethylamine-N-oxide as cardiovascular risk biomarker: A systematic review and dose-response meta-analysis. *Eur. Heart. J.* **38**, 2948-2956 (2017).

14. Tang, W. H. et al. Intestinal microbial metabolism of phosphatidylcholine and cardiovascular risk. *New Eng. J. Med.* **368**, 1575-1584 (2013).

15. Zhu, Y. et al. Carnitine metabolism to trimethylamine by an unusual rieske-type oxygenase from human microbiota. *Proc. Natl. Acad. Sci. U. S. A.* **111**, 4268-4273 (2014).

16. Zhu, W. et al. Gut microbial metabolite tmao enhances platelet hyperreactivity and thrombosis risk. *Cell* **165**, 111-124 (2016).

17. Zhu, W. F., Wang, Z. N., Tang, W. H. W. & Hazen, S. L. Gut microbe-generated trimethylamine n-oxide from dietary choline is prothrombotic in subjects. *Circulation* **135**, 1671-1673 (2017).

18. Koeth, R. A. et al. L-carnitine in omnivorous diets induces an atherogenic gut microbial pathway in humans. *J. Clin. Invest.* **129**, 373-387 (2019).

19. Koeth, R. A. et al. γ-butyrobetaine is a proatherogenic intermediate in gut microbial metabolism of L-carnitine to TMAO. *Cell Metab.* **20**, 799-812 (2014).

20. Wu, W. K. et al. Characterization of TMAO productivity from carnitine challenge facilitates personalized nutrition and microbiome signatures discovery. *Microbiome* **8**, 162 (2020).

21. Barabási, A.-L., Menichetti, G. & Loscalzo, J. The unmapped chemical complexity of our diet. *Nat. Food* **1**, 33-37 (2020).

22. Roberts, A. B. et al. Development of a gut microbe-targeted nonlethal therapeutic to inhibit thrombosis potential. *Nat. Med.* **24**, 1407-1417 (2018).

23. Smits, L. P. et al. Effect of vegan fecal microbiota transplantation on carnitine- and choline-derived trimethylamine-N-oxide production and vascular inflammation in patients with metabolic syndrome. *J. Am. Heart Assoc.* **7**, (2018).

24. Wang, Z. et al. Non-lethal inhibition of gut microbial trimethylamine production for the treatment of atherosclerosis. *Cell* **163**, 1585-1595 (2015).

25. Petrovska, B. B. & Cekovska, S. Extracts from the history and medical properties of garlic. *Pharmacogn. Rev.* **4**, 106-110 (2010).

26. Banerjee, S. K. & Maulik, S. K. Effect of garlic on cardiovascular disorders: A review. *Nutr. J.* **1**, 4 (2002).

27. Liperoti, R., Vetrano, D. L., Bernabei, R. & Onder, G. Herbal medications in cardiovascular medicine. *J. Am. Coll. Cardiol.* **69**, 1188-1199 (2017).

28. Rahman, K. & Lowe, G. M. Garlic and cardiovascular disease: A critical review. *J. Nutr.* **136**, 736-740 (2006).

29. Sobenin, I. A., Pryanishnikov, V. V., Kunnova, L. M., Rabinovich, Y. A., Martirosyan, D. M. & Orekhov, A. N. The effects of time-released garlic powder tablets on multifunctional cardiovascular risk in patients with coronary artery disease. *Lipids Health Dis.* **9**, (2010).

30. Harris, J. C., Cottrell, S. L., Plummer, S. & Lloyd, D. Antimicrobial properties of *Allium sativum* (garlic). *Appl. Microbiol. Biotechnol.* **57**, 282-286 (2001).

31. Ankri, S. & Mirelman, D. Antimicrobial properties of allicin from garlic. *Microbes Infect.* **1**, 125-129 (1999).

32. Choo, S. et al. Review: Antimicrobial properties of allicin used alone or in combination with other medications. *Folia. Microbiol.* **65**, 451-465 (2020).

33. Reiter, J., Levina, N., van der Linden, M., Gruhlke, M., Martin, C. & Slusarenko, A. J. Diallylthiosulfinate (allicin), a volatile antimicrobial from garlic (*Allium sativum*), kills human lung pathogenic bacteria, including MDR strains, as a vapor. *Molecules* **22**, (2017).

34. Panyod, S. & Sheen, L. Y. Beneficial effects of chinese herbs in the treatment of fatty liver diseases. *J. Tradit. Complement. Med.* **10**, 260-267 (2020).

35. Panyod, S. et al. Allicin modifies the composition and function of the gut microbiota in alcoholic hepatic steatosis mice. *J. Agric. Food. Chem.* **68**, 3088-3098 (2020).

36. Wu, W. K., Panyod, S., Ho, C. T., Kuo, C. H., Wu, M. S. & Sheen, L. Y. Dietary allicin reduces transformation of L-carnitine to TMAO through impact on gut microbiota. *J. Funct. Foods* **15**, 408-417 (2015).

37. Wu, W.-K. et al. Identification of TMAO-producer phenotype and host–diet–gut dysbiosis by carnitine challenge test in human and germ-free mice. *Gut* **68**, 1439-1449 (2019).

38. Kasahara, K. et al. Interactions between *Roseburia intestinalis* and diet modulate atherogenesis in a murine model. *Nat Microbiol* **3**, 1461-1471 (2018).

39. Li, J., Lin, S., Vanhoutte, P. M., Woo, C. W. & Xu, A. *Akkermansia muciniphila* protects against atherosclerosis by preventing metabolic endotoxemia-induced inflammation in $ApoE^{-/-}$ mice. *Circulation* **133**, 2434-2446 (2016).

40. Chen, K. et al. Preventive effects and mechanisms of garlic on dyslipidemia and gut microbiome dysbiosis. *Nutrients* **11**, (2019).

41. O'Gara, E. A., Hill, D. J. & Maslin, D. J. Activities of garlic oil, garlic powder, and their diallyl constituents against *Helicobacter pylori*. *Appl. Environ. Microb.* **66**, 2269-2273 (2000).

42. Naganawa, R., Iwata, N., Ishikawa, K., Fukuda, H., Fujino, T. & Suzuki, A. Inhibition of microbial growth by ajoene, a sulfur-containing compound derived from garlic. *Appl. Environ. Microb.* **62**, 4238-4242 (1996).

43. Casella, S., Leonardi, M., Melai, B., Fratini, F. & Pistelli, L. The role of diallyl sulfides and dipropyl sulfides in the in vitro antimicrobial activity of the essential oil of garlic, *Allium sativum* L., and leek, *Allium porrum* L. *Phytother. Res.* **27**, 380-383 (2013).

44. Avato, P., Tursi, F., Vitali, C., Miccolis, V. & Candido, V. Allylsulfide constituents of garlic volatile oil as antimicrobial agents. *Phytomedicine* **7**, 239-243 (2000).

45. Everard, A. et al. Cross-talk between *Akkermansia muciniphila* and intestinal epithelium controls diet-induced obesity. *Proc. Natl Acad. Sci. U. S. A.* **110**, 9066-9071 (2013).

46. Chelakkot, C. et al. *Akkermansia muciniphila*-derived extracellular vesicles influence gut permeability through the regulation of tight junctions. *Exp. Mol. Med.* **50**, (2018).

47. Sokol, H. et al. *Faecalibacterium prausnitzii* is an anti-inflammatory commensal bacterium identified by gut microbiota analysis of crohn disease patients. *Proc. Natl Acad. Sci. U. S. A.* **105**, 16731-16736 (2008).

48. Panyod, S. et al. Diet supplementation with allicin protects against alcoholic fatty liver disease in mice by improving anti-inflammation and antioxidative functions. *J. Agric. Food Chem.* **64**, 7104-7113 (2016).

49. Beattie, J. H., Duthie, S. J., Kwun, I. S., Ha, T. Y. & Gordon, M. J. Rapid quantification of aortic lesions in ApoE$^{(-/-)}$ mice. *J. Vasc. Res.* **46**, 347-352 (2009).

50. Lai, Y. S. et al. Garlic essential oil protects against obesity-triggered nonalcoholic fatty liver disease through modulation of lipid metabolism and oxidative stress. *J. Agric. Food Chem.* **62**, 5897-5906 (2014).

51. Goodman, A. L. et al. Extensive personal human gut microbiota culture collections characterized and manipulated in gnotobiotic mice. *Proc. Natl Acad. Sci. U. S. A.* **108**, 6252-6257 (2011).

52. Krautkramer, K. A. et al. Diet-microbiota interactions mediate global epigenetic programming in multiple host tissues. *Mol. Cell.* **64**, 982-992 (2016).

53. Mortele, O. et al. Optimization of an in vitro gut microbiome biotransformation platform with chlorogenic acid as model compound: From fecal sample to biotransformation product identification. *J. Pharmaceut. Biomed.* **175**, (2019).

54. Romano, K. A., Vivas, E. I., Amador-Noguez, D. & Rey, F. E. Intestinal microbiota composition modulates choline bioavailability from diet and accumulation of the proatherogenic metabolite trimethylamine-N-oxide. *mBio* **6**, e02481 (2015).

55. Wu, W. K. et al. Optimization of fecal sample processing for microbiome study - the journey from bathroom to bench. *J. Formos. Med. Assoc.* **118**, 545-555 (2019).

56. Comeau, A. M., Douglas, G. M. & Langille, M. G. Microbiome helper: A custom and streamlined workflow for microbiome research. *mSystems* **2**, (2017).

57. Rognes, T., Flouri, T., Nichols, B., Quince, C. & Mahe, F. Vsearch: A versatile open source tool for metagenomics. *PeerJ* **4**, e2584 (2016).

58. Caporaso, J. G. et al. Qiime allows analysis of high-throughput community sequencing data. *Nat. Methods* **7**, 335-336 (2010).

Figures

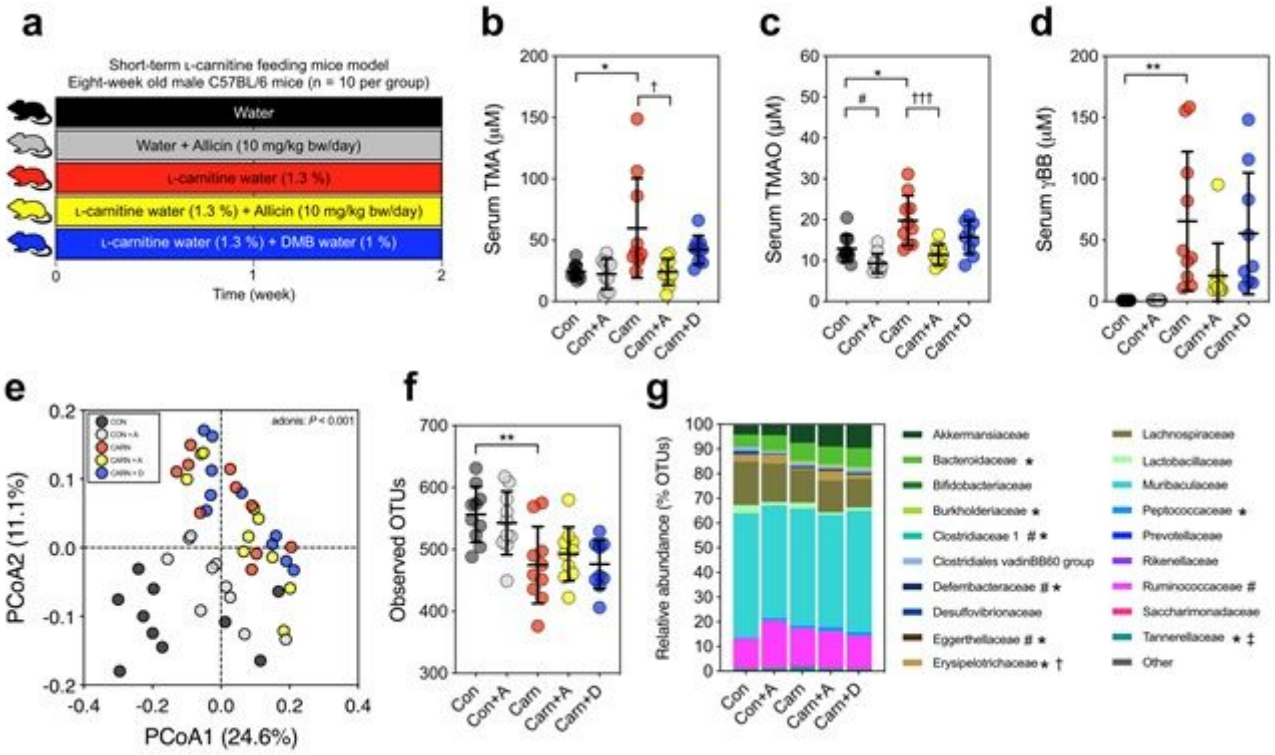

Figure 1

Allicin reduced serum TMA and TMAO, and -carnitine principally changed the fecal microbiome composition in -carnitine-fed male C57BL/6J mice (n=10). (a) Experimental design; (b) serum TMA; (c) serum TMAO; (d) serum γBB; (e) principal coordinate analysis (PCoA) plot with Bray–Curtis dissimilarity; (f) observed OTUs α-diversity indices; and (g) relative abundance of fecal microbiota at family level. Scatter plots are expressed as the mean±SD; Statistical analyses were performed using an unpaired two-tailed Student's t-test control vs control + allicin group (#, $p < 0.05$), control vs carnitine group (*, $p < 0.05$; and **, $p < 0.01$); one-way ANOVA with Tukey's range test for comparisons, carnitine vs carnitine + allicin group (†, $p < 0.05$; and †††, $p < 0.001$). The relative abundance bar plot statistical analyses were performed using an unpaired Wilcoxon signed-rank test with the false discovery rate (FDR), control vs control + allicin group (#, $q < 0.1$); control vs carnitine group (*, $q < 0.1$;); carnitine vs carnitine + allicin group (†, $q < 0.1$); carnitine + DMB group (‡, $q < 0.1$).

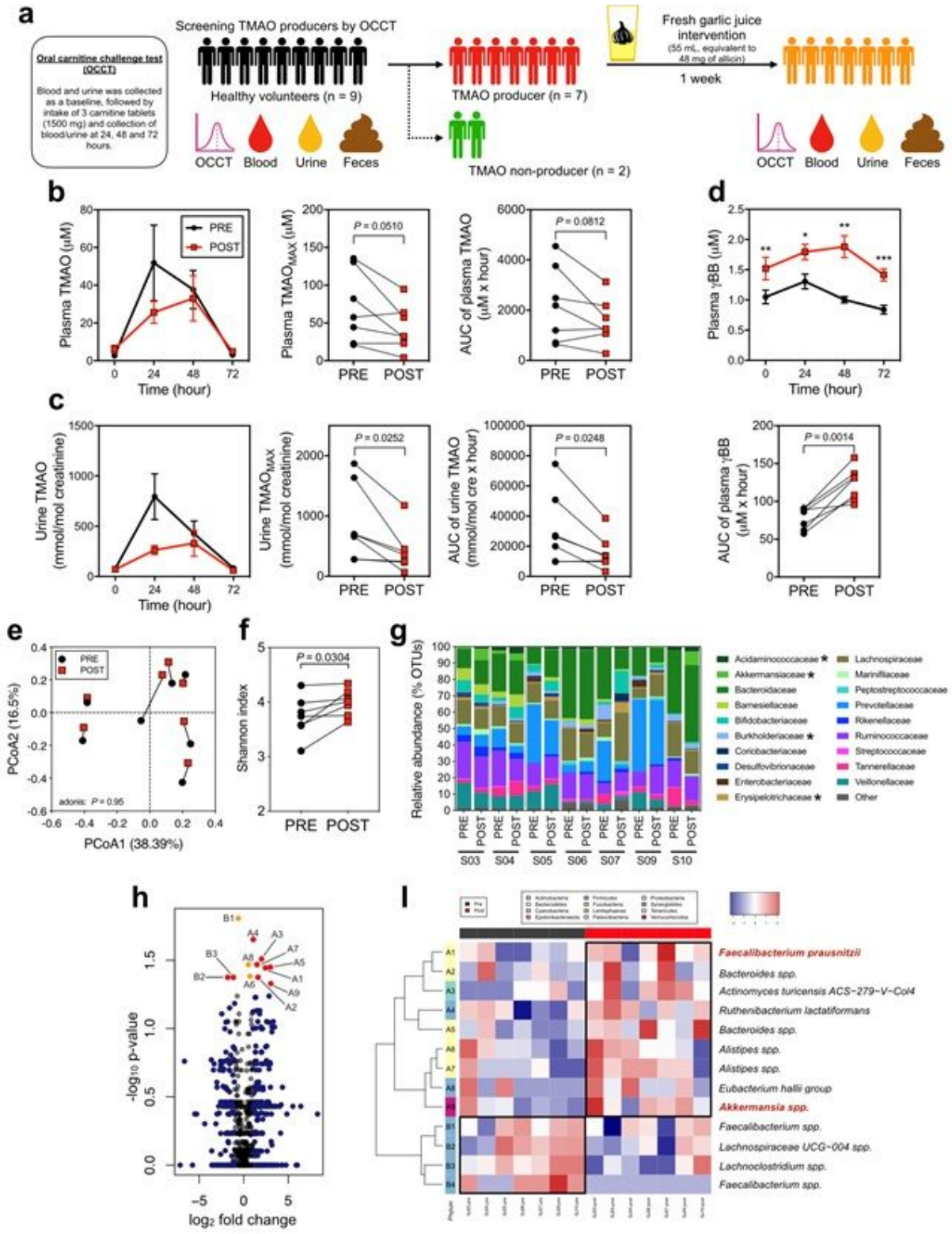

Figure 2

Raw garlic juice reduced plasma TMAO formation ability, increased plasma γBB level in healthy TMAO-producers, and shaped fecal microbiota composition via increasing the evenness, alpha diversity and relative abundance of specific beneficial bacterial taxa. (a) Experimental design, healthy participants (n = 9) were screened for TMAO production using oral carnitine challenge test (OCCT), the criterion for categorization as high-TMAO producers was plasma TMAOMAX > 10 μM. High-TMAO producers (n = 7)

subsequently received an intervention of garlic juice (55 mL, equivalent to 48 mg of allicin/day) for 1 week, followed by OCCT; (b) plasma and (c) urine TMAO, TMAOMAX, and TMAOAUC; (d) plasma γBB and γBBAUC. (e) Principal coordinate analysis (PCoA) plot with Bray–Curtis dissimilarity; (f) Shannon α-diversity index; (g) family-level composition of fecal microbiome; (h) volcano plot of fecal microbiota before and after garlic juice intervention; and (i) heat map of the relative abundances of fecal microbiota with a significant difference using the Wilcoxon signed-rank test ($q < 0.05$). Data are expressed as the mean±SEM; statistical analysis were performed by using two-tailed paired Student's t-test. The relative abundance bar plot statistical analysis was performed using a paired Wilcoxon signed-rank test (*, $p < 0.05$).

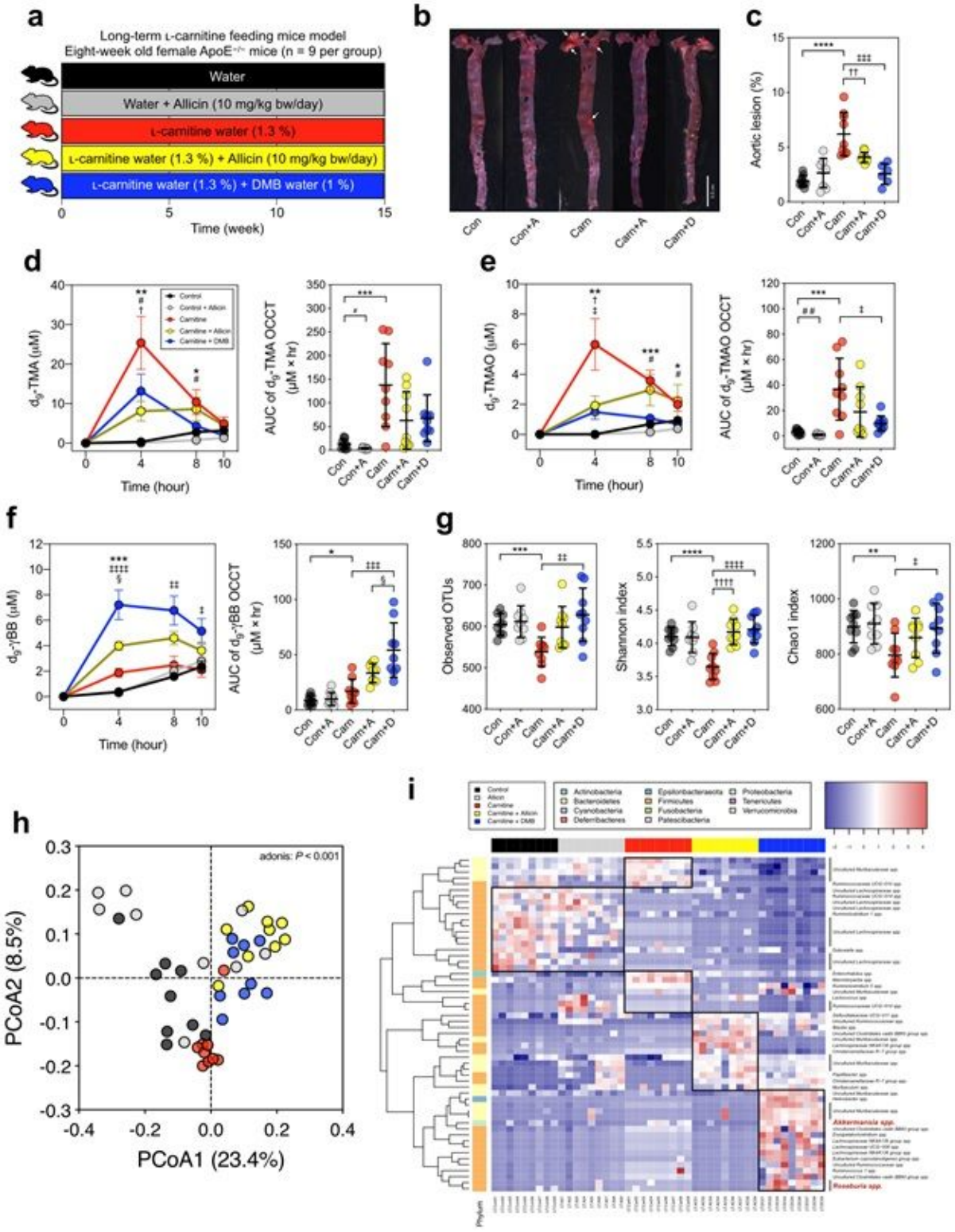

Figure 3

Allicin reduced aortic lesions through the reduction of TMA and TMAO formation and changed the fecal microbiome composition in ⍰-carnitine-induced atherosclerosis female ApoE−/− mice (n=9). (a) experimental design; (b) representative image of oil red-stained aorta; (c) percentage of aortic lesion; (d) d9-TMA level according to oral carnitine challenge test (OCCT) and its AUC; (e) d9-TMAO level of OCCT and its AUC; (f) d9-γBB level according to OCCT and its AUC. (g) α-diversity indices, observed OTUs,

Shannon index and Chao1 index; (h) Principal coordinate analysis (PCoA) plot with Bray–Curtis dissimilarity; and (i) heat map of the relative abundances of fecal microbiota with a significant difference using the Kruskal–Wallis test with false discovery rate (FDR) (q < 0.001). OCCT curves are expressed as the mean±SEM, and scatter plots are expressed as the mean±SD; Statistical analyses were performed using an unpaired two-tailed Student's t-test control vs control + allicin group (#, p < 0.05, and ##, p < 0.01), control vs carnitine group (*, p < 0.05; **, p < 0.01; ***, p < 0.001; and ****, p < 0.0001); one-way ANOVA with Tukey's range test for comparisons, carnitine vs carnitine + allicin group (†, p < 0.05; ††, p < 0.01; and ††††, p < 0.0001), carnitine vs carnitine + DMB group (‡, p < 0.05; ‡‡, p < 0.01; ‡‡‡, p < 0.001; and ‡‡‡‡, p < 0.0001), carnitine + allicin vs carnitine + DMB group (§, p < 0.05).

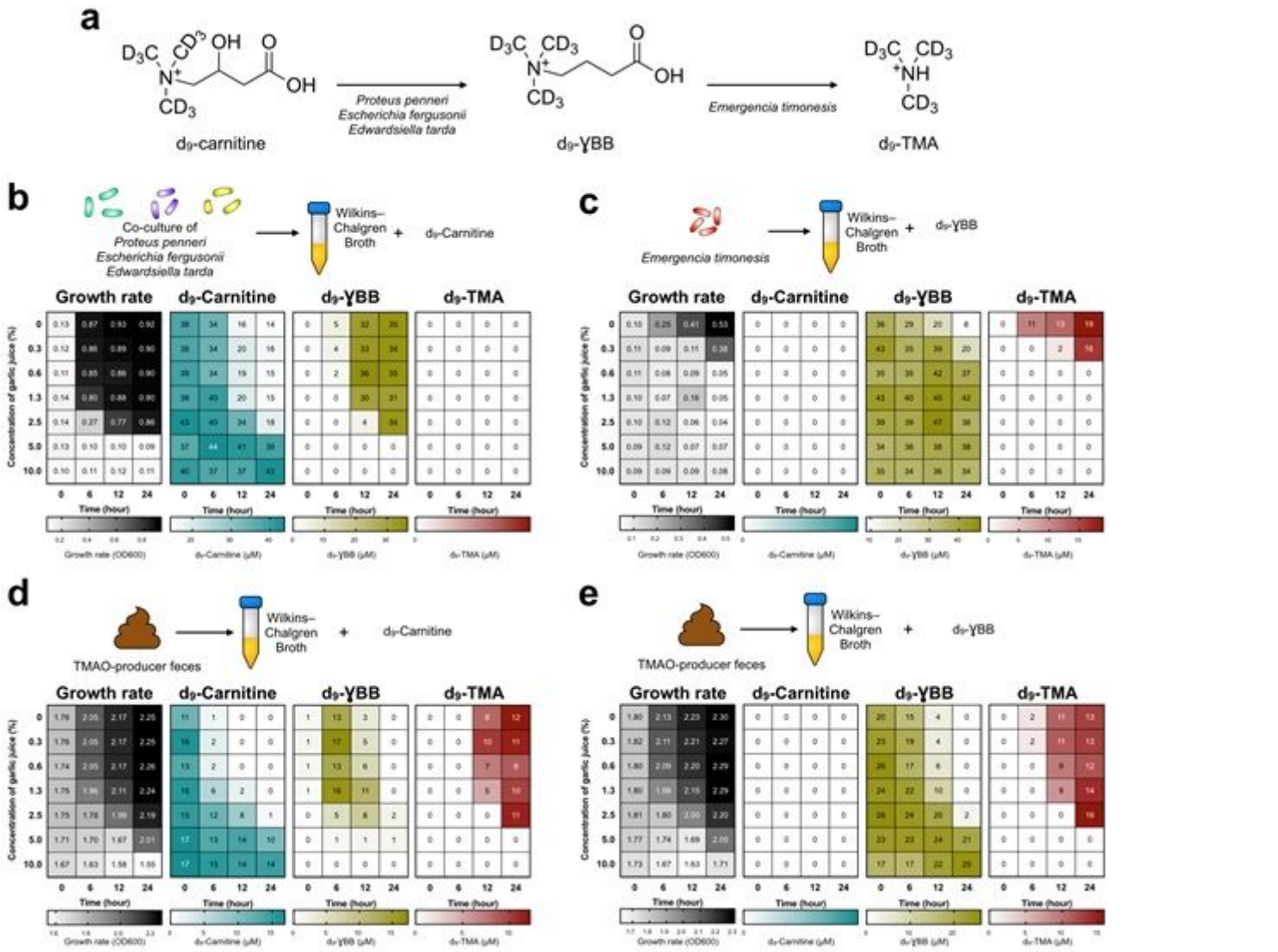

Figure 4

Garlic juice inhibited the formation of d9-TMA and d9-γBB in vitro after inoculation of TMA/γBB-producing bacteria or the feces from high-TMAO producers. (a) Schematic diagram of the bacteria responsible for metabolite d9-carnitine → d9-γBB → d9-TMA; (b) inhibitory effect of garlic juice on carnitine → γBB bacteria (co-culture of Proteus penneri, Escherichia fergusonii, and Edwardsiella tarda) in WC medium supplemented with d9-carnitine; (c) inhibitory effect of garlic juice on the bacteria

responsible for converting γBB to TMA (Emergencia timonensis) in WC medium supplemented with d9-γBB. (d) Inhibitory effect of garlic juice on the high-TMAO-producing gut microbiome in WC medium supplemented with d9-carnitine and (e) d9-γBB.

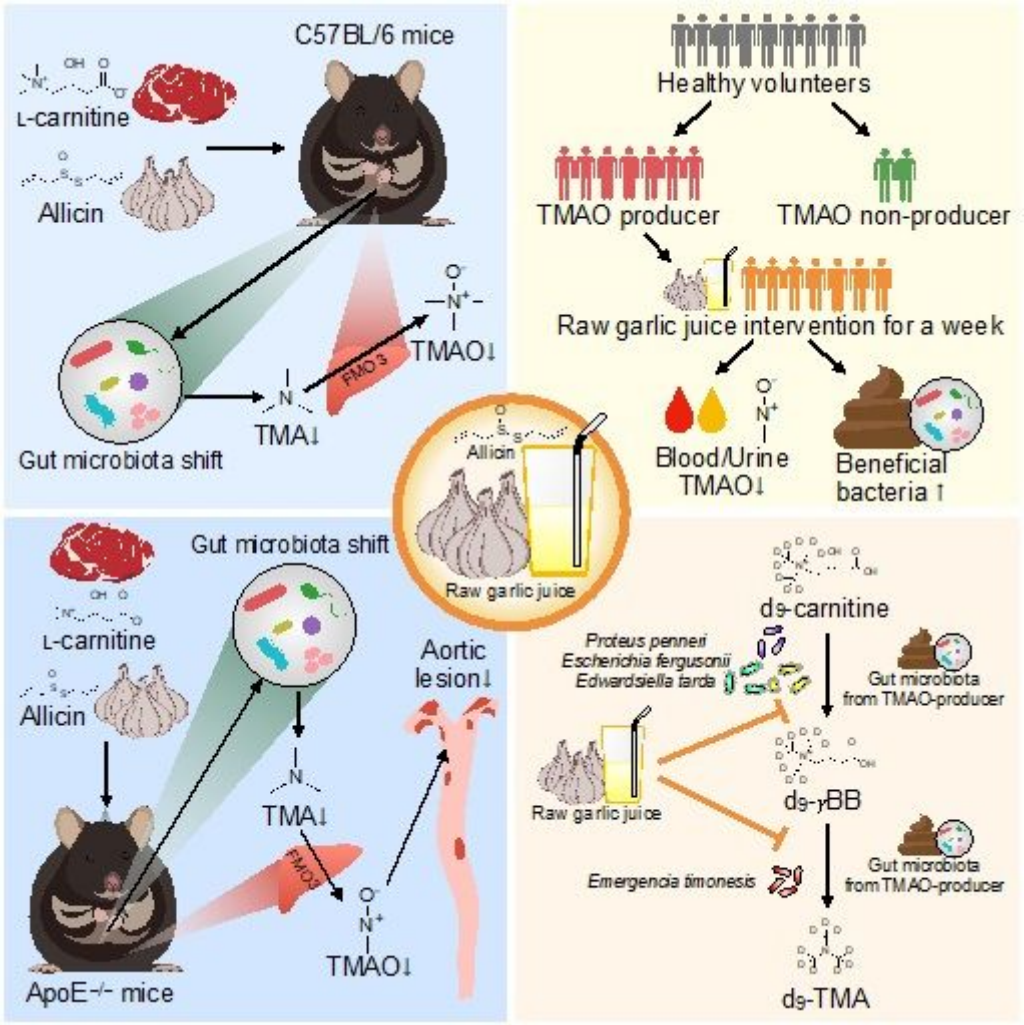

Figure 5

The role of allicin and raw garlic juice on CVD prevention and atherosclerosis amelioration through gut microbiota and TMAO modulation. (1) Allicin decreased gut microbiota and host-derived TMA and TMAO in mice supplemented with -carnitine in drinking water; (2) Raw garlic juice reduced plasma and urine TMAO and increased beneficial gut bacteria in high-TMAO producing humans; (3) Allicin ameliorated aortic lesions by reducing TMA/TMAO production and altered the gut microbiome in -carnitine-induced atherosclerosis ApoE−/− mice; (4) Raw garlic juice inhibited microbial pathway of carnitine → γBB → TMA conversion in specific bacteria and high-TMAO producer's gut microbiome.

Supplementary Files

This is a list of supplementary files associated with this preprint. Click to download.

- Supplementarynpjbiofilmsandmicrobiomes.docx